

## Correlation Analysis of Geomagnetic Parameter with South Atlantic Anomaly Region

Khairul Afi Nasuddin<sup>a</sup>, Mardina Abdullah<sup>a,b</sup> & Nurul Shazana Abdul Hamid<sup>\*</sup>

<sup>a</sup>Department of Electrical, Electronic and System Engineering, Faculty Engineering and Built Environment, Universiti Kebangsaan Malaysia, Malaysia

<sup>b</sup>Space Science Center (ANGKASA), Institute of Climate Change, Universiti Kebangsaan Malaysia, Malaysia

<sup>c</sup>Department of Applied Physics, Faculty of Science and Technology, Universiti Kebangsaan Malaysia, Malaysia

\*Corresponding author: shazana.ukm@gmail.com

Received 7 January 2022, Received in revised form 28 June 2022

Accepted 30 July 2022, Available online 30 January 2023

### ABSTRACT

South Atlantic Anomaly (SAA) region is describe as a region with weak Earth magnetic field. The method apply is power spectrum analysis. By applying the power spectrum analysis method, the value of spectral exponent,  $\beta$  is obtained. From the spectral exponent,  $\beta$ , the Hurst exponent can be determined. The research is conducted by studying the SAA region where comparisons is made between the middle latitude region and high latitude region. 2 active period has been research, 11 March 2011 and 29 May 2011 and 2 normal period has been studied, 9 March 2011 and 12 May 2011. The research conduct indicate the SAA region tend to be persistent and as the vertical field intensity and total field intensity increase, the region tend to have a mixture of antipersistent and persistent characteristic. The high latitude region in this research conduct indicate a tendency to be antipersistent. By conducting research on the SAA region, it can provide knowledge of the dynamics and conditions of our Earth. The SAA region is a region where it is exposed to energetic particles. Satellites passing through the SAA region are also vulnerable to danger. Therefore, the region conducted on the SAA region, can provide knowledge on the characteristics of the SAA region. Research on SAA may increase knowledge of the Earth's magnetic field.

*Keywords:* South Atlantic Anomaly, vertical field intensity, total field intensity

### INTRODUCTION

Technological innovation is the basis for development and advancement in manufacturing design (Oladeji Araoyinbo et al. 2022). With the development of science and technology, it has significant parts of any transportation highway and railway networks (Naser 2022). Construction has been presented in the course history wherever there are human civilization and development— incorporating the usage of environmental resources of land, geography as well as human innovation, skills, and workforce to be utilized for structures in order to serve as welfare and continue needs (Mohammed Hatem et al. 2022). An evaluation of infrastructure concerning capacity and safety is very important since it is directly related to environmental issues (Muhammad & Jamaludin 2022). These, are essential and important elements that ensure safety as well as wellbeing of people and also promote beauty, convenience and aesthetics in the overall built-up environment (Samuel Omoniyi et al. 2022).

In the time domain, many natural phenomena exhibit happen. The Earth's magnetic field is one of the natural phenomena occurring in our life. The trapping and distribution of energetic ionized particles are define by the structure of the Earth's magnetic field (Badhwar 1997). The

Earth's magnetic field assist in deflecting nearly all of the solar wind, which its charged particles is able to strip away the ozone layer that safeguards the planet Earth.

With the evolution of technology, research on the South Atlantic Anomaly (SAA) has been conducted. The SAA is a low intensity magnetic field region that extends across east of Africa over the Atlantic Ocean toward South America (Koch & Kuvshinov 2015). The SAA origin is generally attributed to the offset of the Earth's magnetic dipole. This occurs near the Earth and coincides with a region of intense radiation in space (Heirtzler 2002).

Intense particle precipitation can cover a larger geographical area during magnetic disturbances (Abdu et al. 2005). SAA is an area which the Earth's inner Van Allen radiation belt appears nearest to the Earth's surface. Because of the asymmetry of the geomagnetic field around the Earth's geomagnetic center, the radiation belt particles interact more with the Earth's atmosphere in the area of low field intensity (Jr & Gonzalez 1989). As a result, the SAA has a higher number of energetic particles than other area of space (Jalabert & Mercier 2018).

Energy particles obtained by the geomagnetic field are able to reach lower altitudes, creating a high-radiation region (Zou et al. 2015). This region is further vulnerable toward radiation from high-energy particles. The onboard satellite

oscillator accelerates abnormally due to its sensitivity to this radiation (Willis et al. 2016). Low Earth Orbit space vehicles spend most of the time in the SAA region. The greatest radiation dose impact on spacecraft occurs in this region, which is associated with intense fluxes of charged particles (Grigoryan et al. 2008).

Study on the SAA has been made by Schaefer et al. (2016). The study focusses on the observation and modelling on the South Atlantic Anomaly in low Earth orbit by applying photometric instrument data. In the study, a new model of the SAA particle flux intensity is presented for low Earth orbit. The set of data is based on the particle noise pulses in an ultraviolet photomultiplier. Based on the data set, it can present on a daily basis observing the intensity of the particle radiation on a local time as well as at a fixed altitude. The existence of major doses of radiation experienced in space is one of the potential risks to spacecraft in orbit around the Earth (Schaefer et al. 2016). The model explained is capable to observe along with spatially forecast the changes in particle fluxes perceived by instruments in concurrent low Earth orbits throughout the SAA.

One of the studies on the scaling as well as fractal properties of the horizontal component of the geomagnetic field time series acquired by the Magnetic Data Acquisition System has been done by A. Hamid et al. (2010). The power spectrum method is performed as well as rescaled range analysis and detrended fluctuation analysis. The presence of scaling as indicated by the use of respective fractal methods indicates that the geomagnetic time series under consideration have fractal properties over a wide range of time durations (A. Hamid et al. 2010). The outcome of this research imply that the horizontal geomagnetic field on these stations happen to be fractal in nature in addition to persistent.

The research of South-Atlantic Anomaly magnetic storms effects as observed outside the International Space Station (ISS) in 2008-2016 has been conducted by Dachev (2018). The data are gather in 3 different periods from 2008 to 2016 at 3 ESA EXPOSE platform missions (Dachev 2018). Two Liulin kind spectrometers carry out calculation of the energetic particles flux outside the ISS. The method apply is linear regression analysis. The data show the SAA flux dependency from the Joule heating in the neutral atmosphere density and high latitudes is permanent and is a continues process having an effect on the SAA fluxes all the time.

Volcanoes are complex dynamical structures governed by interactions between a variety of mechanisms, with the most dramatic effects occurring near eruptive events (Currenti et al. 2005). The hourly means of the local geomagnetic field reported at Mt. Etna volcano were subjected to the Multifractal Detrended Fluctuation Analysis (MF-DFA), which allows for the detection of multifractality in nonstationary signals (southern Italy). The research looked at the signal from a geomagnetic station on the

summit of a volcano that had a powerful eruption on October 27, 2002. The results reveal that the geomagnetic time series generates multifractal and the signal's multifractal degree decreases after an eruption.

For this research, comparison will be made between the SAA region and the middle latitude region as well as the high latitude region. Study applying power spectrum analysis will be done to compare the characteristic of the SAA region and other region outside the SAA during normal period indicated as the period where no occurrence of geomagnetic storm and active period referring to period where the occurrence of the geomagnetic storm happen.

METHODOLOGY

STATIONS

The location of study is display in figure 1. The red color represents the South Atlantic Anomaly region. The green color represents the middle latitude region. The blue color is for the high latitude region. Figure 1 represent the station in the research. The station-station is place by its region.

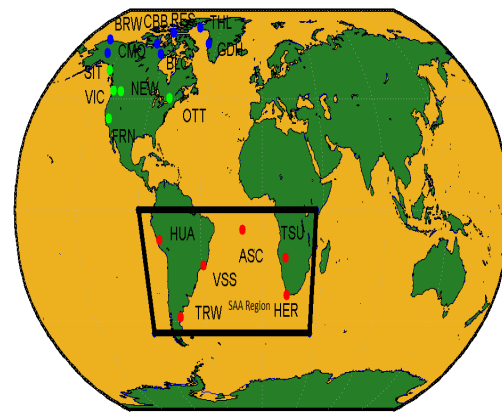


FIGURE 1. The location of study in the research

The station involve in the region is display in Table 1, 2 and 3. It consists of stations in the SAA region, middle latitude region and high latitude region.

TABLE 1. Stations in the SAA region (C. Finlay et al. 2020)

Station Name	IAGA Code	Geodetic Latitude	Geodetic Longitude
Hermanaus	HER	-34.425	19.225
Ascension Island	ASC	-7.949	345.624
Huancayo	HUA	-12.038	284.682
Vassouras	VSS	-22.400	316.400
Tsumeb	TSU	-19.202	17.584
Trelew	TRW	-43.266	294.617

TABLE 2. Stations in the middle latitude region

Station Name	IAGA Code	Geodetic Latitude	Geodetic Longitude
Fresno	FRN	37.091	240.279
Ottawa	OTT	45.403	284.447
Newport	NEW	48.271	242.880
Sitka	SIT	57.061	224.669
Victoria	VIC	48.517	236.582

TABLE 3. Stations in the high latitude region

Station Name	IAGA Code	Geodetic Latitude	Geodetic Longitude
Cambridge Bay	CBB	69.123	254.968
Baker Lake	BLC	64.319	263.988
Thule	THL	77.470	290.770
Barrow	BRW	71.320	203.380
Godhavn	GDH	69.250	306.470
Resolute Bay	RES	74.690	265.105
College	CMO	64.871	212.139

#### THE H-COMPONENT OF THE EARTH MAGNETIC FIELD AND POWER SPECTRUM ANALYSIS

The horizontal magnetic field lines in the equator create a unique current system as mentioned (Abdul Hamid et al. 2014). The horizontal component is chosen since it sensitive to geomagnetic activeness. After choosing the horizontal component, it is examine using power spectrum analysis. Figure 2 is an example figure for power spectral density. The periodogram is obtained from station ASC on 29 May 2011.

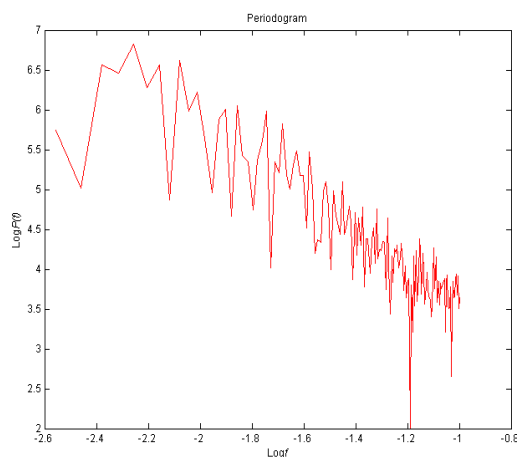


FIGURE 2. The power spectral density

$S_m$  which represent the power spectral density function, on behalf of a discrete time series, denoted by  $y_n$ , where  $n = 1, 2, 3, \dots, N$  can be formulated as (D. Malamud & L. Turcotte 1999).

$$S_m = \lim_{N \rightarrow \infty} \left\{ \frac{2|y_m|^2}{N\delta} \right\}, m = 1, 2, 3, \dots, \frac{N}{2}, \quad (1)$$

It is to be noted that  $\delta$  is the time amongst sequential  $n$ . The power spectrum is applied since it can indicate the power of each frequency component of the source time domain waveform. It can also be applied to analyze variety of physiological signals.

The concept and use of the power spectrum of a signal is fundamental in the field of electrical engineering. This is particularly in the electronic communication systems such as radars, radio communications as well as related systems.

The spectral analysis of a time series can be able for one to understand something concerning the characteristic time scales of an occurrence which contribute to the development of the observed variations. On behalf of a self-affine time series,  $S_m$  designated as the power-spectral density is depicted to include a power-law dependence on frequency (Nasuddin et al. 2019)

$$S_m \sim f_m^{-\beta}, m = 1, 2, 3, \dots, \frac{N}{2}, \quad (2)$$

which by  $f_m = m/N$ . It is to be define the value of  $\beta$  is a measure of the intensity of persistence in a time series.

#### HURST EXPONENT, ANTIPERSISTENT, PERSISTENT AND RANDOM NOISE

The value of  $\beta$  is apply in order to determine the Hurst exponent. When  $1 < \beta < 3$ , the method to calculate the Hurst exponent is . On the other hand, when  $-1 \leq \beta < 1$ , the approach is .

The Hurst exponent,  $H$ , will be used to identify the correlation and classify a time series, with values ranging from 0 to 1 (Abdul Hamid et al. 2009). For  $0 < H < 0.5$ , it is called antipersistent. A positive anomaly in the past is more likely to be followed by a negative anomaly in the future and conversely for antipersistent processes (Panchev & Tsekov 2007). For  $0.5 < H < 1$ , it is known as persistent. It imply a positive or negative anomaly in the past is further likely to be followed by the same type of anomaly in the future. For  $H = 0.5$ , it indicate a random series.

#### ACTIVE PERIOD AND NORMAL PERIOD

For this period, the active period and normal period is chosen on year 2011. The active period is the period when occurrence of geomagnetic storm occur and the normal period is the period when no geomagnetic storm occur. Figure 3 indicate the Dst Index for 10 March 2011 which show the development on the geomagnetic storm only after 9 UT. Before this period on 10 March 2011, no geomagnetic storm existence occurs. While the Dst Index for 11 March 2011 indicate the definition of active period

where geomagnetic storm occurs from 1 UT until 24 UT on that day.

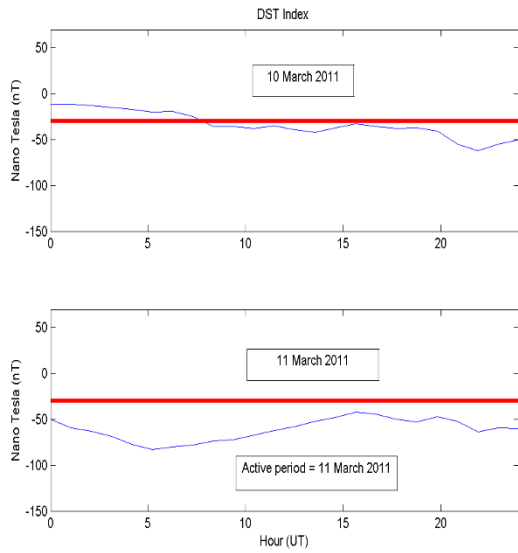


FIGURE 3. The active period on 11 March 2011

Year 2011 is analyzed to study the active period and normal period during the ascending phase of solar cycle 24. In this period, 4 date are chosen. Table 4 indicate the active period and normal period in this research.

TABLE 4. Active period and normal period

Active Period	Normal Period
11 March 2011	9 March 2011
29 May 2011	12 May 2011

Figure 4 indicate the Dst Index for active period and normal period.

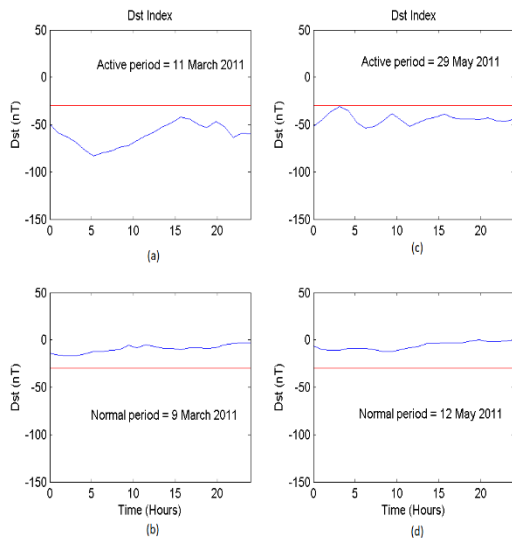


FIGURE 4. Dst Index (a) 11 March 2011 (b) 9 March 2011 (c) 29 May 2011 (d) 12 May 2011

The primary disturbances for the space environment are commonly agreed to be geomagnetic disturbances (Jr et al. 1992). Solar drives such as coronal mass ejections, solar flares, fast streams, and others cause magnetospheric storms, which are sources of geomagnetic activity (Zaourar et al. 2013). A strong magnetic storm sparked an energy blackout for around 50,000 people in Sweden for a short amount of time (November 2003) (Papa & Sosman 2008). For this research, the active period is a period where the event of the geomagnetic storm appears. The normal period is a period where no geomagnetic storm occurred. Active period are on 11 March 2011 and 29 May 2011. Normal period are on 9 March 2011 and 12 May 2011.

RESULTS AND DISCUSSION

Table 5 and 6 indicate the SAA region for active period, 11 March 2011 and 29 May 2011 as well as normal period, 9 March 2011 and 12 May 2011.

Table 5 and 6 describe the SAA region attribute during active period and normal period. During active period, 11 March 2011 and active period, 29 May 2011, the attribute of the SAA region is analyze. The stations in the SAA region during the active period is reveal to tend to be persistent. In the normal period, 9 March 2011 and normal period, 12 May 2011, the same attribute is being exhibit by the SAA region in this research. Figure 5 indicate the percentage of the SAA region which display 100 % persistent during both active period and normal period.

Based on the analysis, in 11 March 2011, the active period, station VSS indicate a Hurst exponent of  $0.6937 \pm 0.0683$ , station HUA with  $0.5597 \pm 0.0634$ , station HER with  $0.5871 \pm 0.0613$ , station ASC with  $0.6232 \pm 0.0519$  and station TSU with  $0.6002 \pm 0.0569$ . All the station during 11 March 2011 in the SAA region is persistent in this research.

During 9 March 2011, station VSS, station HUA, station HER, station ASC and station TSU is persistent with Hurst exponent of  $0.7062 \pm 0.0548$  for station VSS,  $0.7551 \pm 0.0731$  for station HUA,  $0.6035 \pm 0.0582$  for station HER,  $0.7630 \pm 0.0638$  for station ASC and  $0.7426 \pm 0.0625$  for station TSU.

The characteristic of SAA region tends to be persistent. Similar characteristic is represented in the active period, 29 May 2011 and 12 May 2011 for stations in the SAA region. In the active period, 29 May 2011, station TRW exhibit a Hurst exponent of  $0.7680 \pm 0.0725$ , other station such as station HER with  $0.8834 \pm 0.0696$ , station TSU with  $0.8015 \pm 0.0623$ , station ASC with  $0.5483 \pm 0.0520$  and station HUA with  $0.7457 \pm 0.0693$ . In the normal period, 12 May 2011, the station in the SAA region tends to be persistent with station TRW exhibiting a Hurst exponent of  $0.5271 \pm 0.0585$ , station HER with  $0.6530 \pm 0.0689$ , station TSU with  $0.5168 \pm 0.0616$ , station ASC with  $0.5795 \pm 0.0655$  and station HUA with  $0.6331 \pm 0.0658$ .

The research conducted analysis that the mean of total field intensity is low within the range of 29650 nT experience

by station TSU during normal period, 9 March 2011 and station VSS with 23310 nT during active period, 11 March 2011. The vertical intensity is also low within the range of 144.7 nT experience by station HUA during active period,

9 March 2011 and -25950 nT experience by station TSU during active period, 11 March 2011. It is seen the low total field intensity as well as low vertical intensity may influence the SAA region to tend to be persistent in this research.

TABLE 5. SAA region for 11 March 2011 and 9 March 2011

Station	Hurst exponent value	Mean Total Field Strength Intensity (nT)	Mean Vertical Field Strength Intensity (nT)	Hurst Exponent value	Mean Total Field Strength Intensity (nT)	Mean Vertical Field Strength Intensity (nT)
VSS	$0.6937 \pm 0.0683$	23310	-14050	$0.7062 \pm 0.0548$	23350	-14040
HUA	$0.5597 \pm 0.0634$	25280	138.9	$0.7551 \pm 0.0731$	25340	144.7
HER	$0.5871 \pm 0.0613$	25770	-23500	$0.6035 \pm 0.0582$	25780	-23490
ASC	$0.6232 \pm 0.0519$	28320	-19230	$0.7630 \pm 0.0638$	28360	-19230
TSU	$0.6002 \pm 0.0569$	29630	-25950	$0.7426 \pm 0.0625$	29650	-25940

TABLE 6. SAA region for 29 May 2011 and 12 May 2011

Station	Hurst exponent value	Mean Total Field Strength Intensity (nT)	Mean Vertical Field Strength Intensity (nT)	Hurst Exponent value	Mean Total Field Strength Intensity (nT)	Mean Vertical Field Strength Intensity (nT)
TRW	$0.7680 \pm 0.0725$	25800	-17620	$0.5271 \pm 0.0585$	28360	-19240
HER	$0.8834 \pm 0.0696$	25760	-23480	$0.6530 \pm 0.0689$	25770	-23480
TSU	$0.8015 \pm 0.0623$	29630	-25940	$0.5168 \pm 0.0616$	29640	-25940
ASC	$0.5483 \pm 0.0520$	28340	-19250	$0.5795 \pm 0.0655$	28360	-19240
HUA	$0.7457 \pm 0.0693$	25310	140.4	$0.6331 \pm 0.0658$	25330	138.7

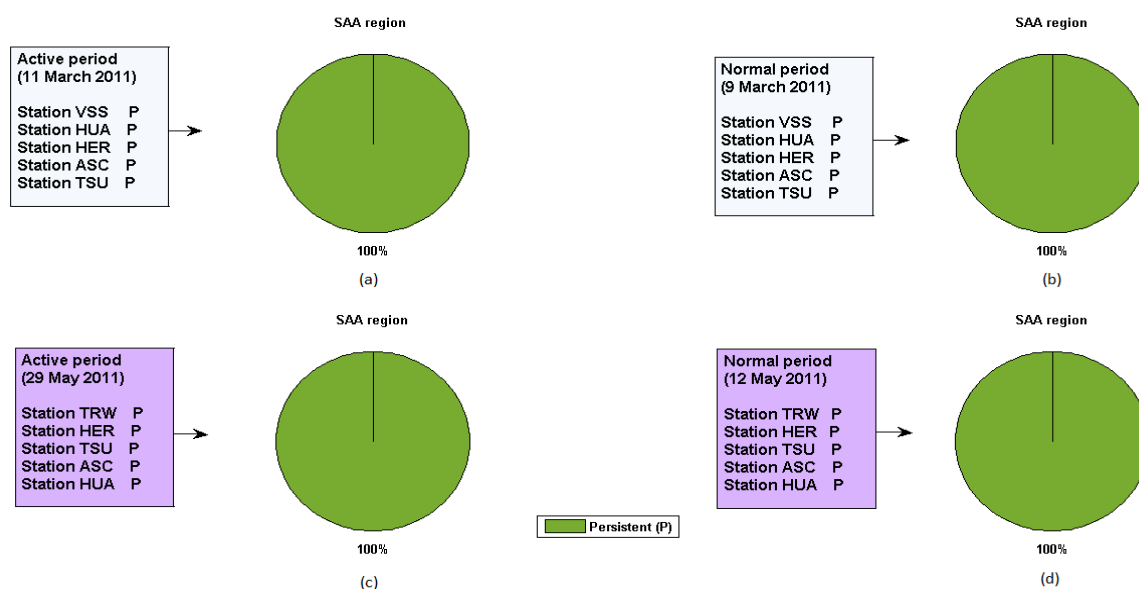


FIGURE 5. Pie chart of SAA region (a) 11 March 2011 (b) 9 March 2011 (c) 29 May 2011 (d) 12 May 2011

Other possible factor to be consider is the ring current. The injection of ions from the solar wind as well as the terrestrial ionosphere may develop the ring current. A geomagnetic storm happen, causing energy content of the ring current to unusually high levels (Kozyra & Liemohn 2003). Following the substorm onsets, energetic particles are injected into the ring current, enhancing the ring current (Huang et al. 2004). Positive ions with energies ranging from -1 keV to a few hundred keV are the primary carriers of the storm ring current. This may also influence the H component of geomagnetic field in the SAA region to produce a tendency to be persistent.

For persistent value, it indicate a positive or negative anomaly in the past is further likely to be followed by the same type of anomaly in the future. The potential for SAA region to tend to have a large number of energetic particle in the SAA region may occur based on the SAA region inclination to be persistent.

Therefore, charged particle in this region are able to cause danger to spacecraft. Cases such as the SAA influencing the Doppler satellite data causing systematic positioning inaccuracies can provide an example. Safety precaution are required when orbiting the SAA region. This can avoid danger to equipment and astronaut which go through the SAA region.

The middle latitude region is analyzed during active period, 11 March 2011 and 29 May 2011 and normal period, 9 March 2011 and 12 May 2011. The research conducted indicate the middle latitude region has different attribute compare to the SAA region. The middle latitude region start to appear antipersistent and this may be due to the increase of total field intensity and vertical field intensity. This can be seen in figure 6. During active period, 11 March 2011, about 80 % characteristic is persistent and 20 % is antipersistent. On the normal period, 9 March 2011, 80 % characteristic is represent with a persistent characteristic and 20 % is experience antipersistent. In the active period, 29 May 2011, 100 % characteristic is persistent while on the normal period, 12 May 2011, 60 % is antipersistent and 40 % produce a persistent characteristic.

During active period, 11 March 2011, 5 station are studied. The appearance of antipersistent occur on station SIT with Hurst exponent of  $0.3571 \pm 0.0622$ . Other station such as station FRN ( $0.6028 \pm 0.0508$ ), station VIC ( $0.6783 \pm 0.0722$ ), station NEW ( $0.6075 \pm 0.0639$ ) and station OTT ( $0.6230 \pm 0.0587$ ) exhibit a persistent attribute.

On the normal period, 9 March 2011, station SIT is antipersistent with Hurst exponent of  $0.4390 \pm 0.0677$ . Station FRN ( $0.6405 \pm 0.0647$ ), station VIC ( $0.6924 \pm 0.0700$ ), station NEW ( $0.6662 \pm 0.0691$ ) and station

OTT ( $0.5474 \pm 0.0610$ ) is persistent in this research. It is examine the total field intensity and vertical field intensity is different in contrast to the SAA region.

In 29 May 2011, the station examine is station FRN with Hurst exponent of  $0.8008 \pm 0.0703$ , station OTT with Hurst exponent of  $0.8308 \pm 0.0679$ , station SIT with Hurst exponent of  $0.6198 \pm 0.0634$ , station NEW with Hurst exponent of  $0.5930 \pm 0.0605$  and station VIC with Hurst exponent of  $0.6212 \pm 0.0714$ .

On the normal period, 12 May 2011, station FRN ( $0.4639 \pm 0.0792$ ), station OTT ( $0.4784 \pm 0.0744$ ) and station SIT ( $0.2603 \pm 0.0748$ ) exhibit an antipersistent while station NEW and VIC is examine to be persistent with Hurst exponent of  $0.5345 \pm 0.0703$  and  $0.5242 \pm 0.0604$ .

The middle latitude experience a mixture of antipersistent and persistent attribute. This may be due to increase of total field intensity. It is observe the range of total field intensity is higher compare to the SAA region with the lowest exhibit by station FRN with 48790 nT during active period, 29 May 2011, the highest with station SIT with 56060 nT on normal period, 9 Mac 2011.

The increase of vertical intensity is seen to occur, this may affect the middle latitude region. It is indicate the lowest vertical intensity is exhibit by station FRN (42720 nT) on active period, 29 May 2011 and normal period, 12 May 2011. The highest vertical intensity is experience by station SIT (53780 nT) on 11 March 2011 (active period) as well as 9 March 2011 (normal period).

The study on the characteristic of the high latitude region is conducted. It is examine the high latitude region tend to be antipersistent different than the middle latitude region and SAA region in this research. Figure 7 identify the characteristic of the high latitude region based on percentage. On active period, 11 March 2011, the high latitude region experience a 40 % antipersistent characteristic and 60 % persistent characteristic. On 9 March 2011, the normal period, about 80 % of the high latitude region experience antipersistent characteristic and 20 % is persistent. On 29 May 2011, the active period, 60 % of the high latitude region is antipersistent and 40 % is persistent. In the normal period, 12 May 2011, the high latitude region indicate a tendency to be antipersistent with 80 % antipersistent and 20 % persistent.

On 11 March 2011, active period, station CMO and station GDH produce an antipersistent characteristic. The Hurst exponent is  $0.4116 \pm 0.0601$  for station CMO and  $0.2840 \pm 0.0379$  for station GDH. Other station such as station THL, station RES and station BLC produce Hurst exponent of  $0.5303 \pm 0.0595$ ,  $0.5936 \pm 0.0669$  and  $0.6466 \pm 0.0878$ .

TABLE 7. Middle latitude region for 11 March 2011 and 9 March 2011

Station	Hurst exponent value	Mean Total Field Strength Intensity (nT)	Mean Vertical Field Strength Intensity (nT)	Hurst Exponent value	Mean Total Field Strength Intensity (nT)	Mean Vertical Field Strength Intensity (nT)
FRN	$0.6028 \pm 0.0508$	48790	42740	$0.6405 \pm 0.0647$	48800	42740
VIC	$0.6783 \pm 0.0722$	54270	50870	$0.6924 \pm 0.0700$	54270	50860
NEW	$0.6075 \pm 0.0639$	55240	52190	$0.6662 \pm 0.0691$	55240	52180
SIT	$0.3571 \pm 0.0622$	56050	53780	$0.4390 \pm 0.0677$	56060	53780
OTT	$0.6230 \pm 0.0587$	54940	51900	$0.5474 \pm 0.0610$	54940	51890

TABLE 8. Middle latitude region for 29 May 2011 and 12 May 2011

Station	Hurst exponent value	Mean Total Field Strength Intensity (nT)	Mean Vertical Field Strength Intensity (nT)	Hurst Exponent value	Mean Total Field Strength Intensity (nT)	Mean Vertical Field Strength Intensity (nT)
FRN	$0.8008 \pm 0.0703$	48770	42720	$0.4639 \pm 0.0792$	48780	42720
OTT	$0.8308 \pm 0.0679$	54910	51850	$0.4784 \pm 0.0744$	54920	51860
SIT	$0.6198 \pm 0.0634$	56010	53740	$0.2603 \pm 0.0748$	56050	53770
NEW	$0.5930 \pm 0.0605$	55210	52150	$0.5345 \pm 0.0703$	55220	52150
VIC	$0.6212 \pm 0.0714$	54240	50840	$0.5242 \pm 0.0604$	54250	50840

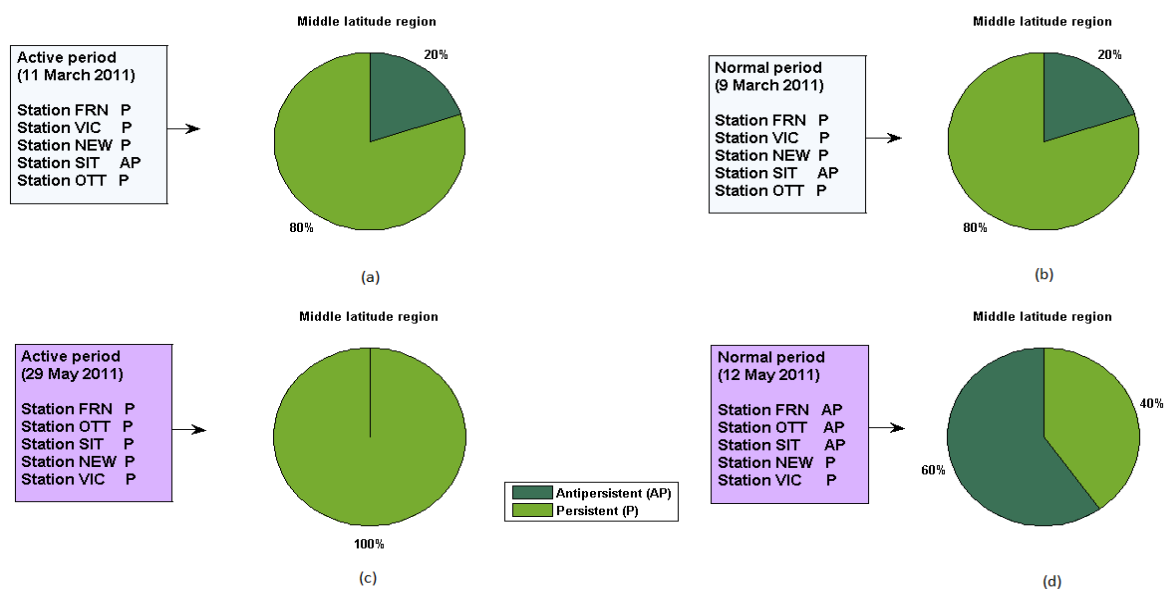


FIGURE 6. Pie chart of Middle latitude region (a) 11 March 2011 (b) 9 March 2011 (c) 29 May 2011 (d) 12 May 2011

On the normal period, 9 March 2011, most of the station produce an antipersistent characteristics. Station CMO (  $0.1308 \pm 0.0669$  ), station GDH (  $0.4800 \pm 0.0641$  ), station RES (  $0.4451 \pm 0.0563$  ) and station BLC (  $0.3579 \pm 0.0586$  ) present an antipersistent characteristic. Other station, station THL is persistent with Hurst exponent of  $0.5692 \pm 0.0794$ .

On 29 May 2011, active period and 12 May 2011, normal period, most of the station in the high latitude region tend to be antipersistent in this research. During 29 May 2011, station BRW (  $0.3896 \pm 0.0752$  ), station GDH (  $0.4785 \pm 0.0662$  ) and station CBB (  $0.3204 \pm 0.0586$  ) indicate antipersistent value. Other station, station RES and station THL produce persistent attribute with Hurst exponent of  $0.6195 \pm 0.0710$  and  $0.8307 \pm 0.0756$ .

During normal period, 12 May 2011, station BRW (  $0.3959 \pm 0.0715$  ), station GDH (  $0.3955 \pm 0.0692$  ), station CBB (  $0.2224 \pm 0.0736$  ) and station RES (  $0.3900 \pm 0.0701$  ) exhibit antipersistent value while station THL is persistent with Hurst exponent,  $0.5542 \pm 0.0624$ .

The high latitude region tend to be antipersistent in contrast to the SAA region and middle latitude region due to the high total field intensity and an increase in vertical intensity. Station BLC indicate a total field intensity of 59180 nT, the highest in the study during 11 March 2011, active period and the lowest total field intensity by station THL with 56420 nT on normal period, 9 March 2011 and 12 May 2011.

The vertical intensity in the high latitude region is also increase with the highest on 11 March 2011, active period with station BLC ( 58840 nT ) and the lowest with station CMO ( 55420 nT ) on 11 March 2011, active period.

Other factor which may cause the major part of antipersistent in the high latitude region experience in this research may be due to the high latitude ionosphere which is influence by the energy sources of magnetospheric origin. In addition, the more vertical magnetic field, it contributes strong magnetospheric-ionospheric coupling in the high latitudes.

TABLE 9. High latitude region for 11 March 2011 and 9 March 2011

Station	Hurst exponent value	Mean Total Field Strength Intensity (nT)	Mean Vertical Field Strength Intensity (nT)	Hurst Exponent value	Mean Total Field Strength Intensity (nT)	Mean Vertical Field Strength Intensity (nT)
CMO	$0.4116 \pm 0.0601$	56810	55420	$0.1308 \pm 0.0669$	56950	55530
GDH	$0.2840 \pm 0.0379$	56580	55890	$0.4800 \pm 0.0641$	56520	55820
THL	$0.5303 \pm 0.0595$	56430	56290	$0.5692 \pm 0.0794$	56420	56280
RES	$0.5936 \pm 0.0669$	57880	57830	$0.4451 \pm 0.0563$	57850	57810
BLC	$0.6466 \pm 0.0878$	59180	58840	$0.3579 \pm 0.0586$	59110	58760

TABLE 10. High latitude region for 29 May 2011 and 12 May 2011

Station	Hurst exponent value	Mean Total Field Strength Intensity (nT)	Mean Vertical Field Strength Intensity (nT)	Hurst Exponent value	Mean Total Field Strength Intensity (nT)	Mean Vertical Field Strength Intensity (nT)
BRW	$0.3896 \pm 0.0752$	57490	56770	$0.3959 \pm 0.0715$	57480	56750
GDH	$0.4785 \pm 0.0662$	56550	55850	$0.3955 \pm 0.0692$	56540	55840
CBB	$0.3204 \pm 0.0586$	58950	58780	$0.2224 \pm 0.0736$	58890	58730
RES	$0.6195 \pm 0.0710$	57870	57820	$0.3900 \pm 0.0701$	57810	57760
THL	$0.8307 \pm 0.0756$	56440	56290	$0.5542 \pm 0.0624$	56420	56270

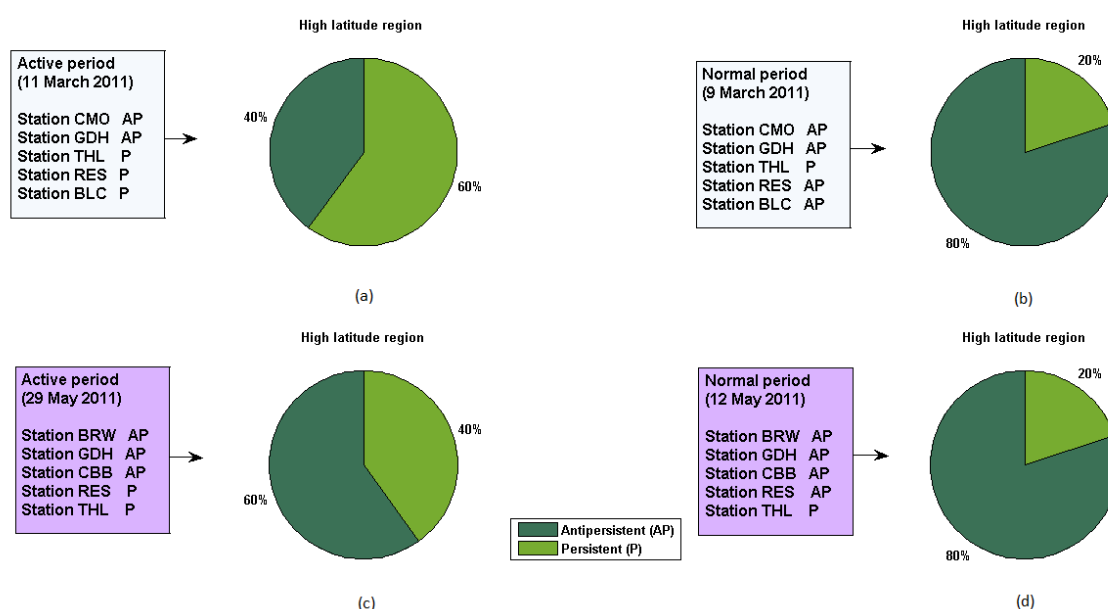


FIGURE 7. Pie chart of High latitude region (a) 11 March 2011 (b) 9 March 2011 (c) 29 May 2011 (d) 12 May 2011

#### CONCLUSION

Based on the research, the SAA region tend to be persistent during active period, 11 March 2011 and 29 May 2011 and normal period, 9 March 2011 and 12 May 2011. The middle latitude region has a different characteristic with a mixture of persistent and antipersistent. The high latitude region tends to be antipersistent compare to the SAA region and middle latitude region. The analysis on the total field intensity and vertical intensity is also done where the SAA region in this research has a low total field intensity and vertical intensity in contrast to the middle latitude region and high latitude region. As the total field intensity and vertical intensity increase, antipersistent characteristic start to appear. As the total field intensity and vertical intensity is higher, the region tends to be antipersistent.

#### ACKNOWLEDGEMENT

The results presented in this paper rely on data collected at magnetic observatories. We thank the national institutes that support them and INTERMAGNET for promoting high standards of magnetic observatory practice ([www.intermagnet.org](http://www.intermagnet.org))

#### DECLARATION OF COMPETING INTEREST

None

#### REFERENCES

- A. Hamid, N.S., Gopir, G., Ismail, M., Misran, N., Usang, M.D. & Yumoto, K. 2010. Scaling and fractal properties of the horizontal geomagnetic field at the Tropical Stations of Langkawi and Davao in February 2007. *AIP Conference Proceedings* 1250: 516–519.
- Abdu, M.A., Batista, I.S., Carrasco, A.J. & Brum, C.G.M. 2005. South Atlantic magnetic anomaly ionization: A review and a new focus on electrodynamic effects in the equatorial ionosphere. *Journal of Atmospheric and Solar-Terrestrial Physics* 67(17–18): 1643–1657.
- Abdul Hamid, N.S., Gopir, G., Ismail, M., Misran, N., Hasbi, A.M., Usang, M.D. & Yumoto, K. 2009. The Hurst exponents of the Geomagnetic Horizontal Component during Quiet and Active Periods. *2009 International Conference on Space Science and Communication, IconSpace - Proceedings* hlm. 186–190
- Abdul Hamid, N.S., Liu, H., Uozumi, T., Yumoto, K., Veenadhari, B., Yoshikawa, A. & Jairo Avendaño Sanchez. 2014. Relationship between the equatorial electrojet and global Sq currents at the dip equator region. *Earth Planets and Space* 66: 1–11.
- Badhwar, G.D. 1997. Drift rate of the South Atlantic Anomaly. *Journal of Geophysical Research* 102(A2): 2343–2349.
- C. Finlay, C., Kloss, C., Olsen, N., D. Hammer, M., Toffner-Clausen, L., Grayver, A. & Kuvshinov, A. 2020. The CHAOS-7 geomagnetic field model and observed changes in the South Atlantic Anomaly. *Earth, Planets and Space* 72: 1–31.
- Currenti, G., Negro, C. del, Lapenna, V. & Telesca, L. 2005. Multifractality in local geomagnetic field at Etna volcano, Sicily (southern Italy). *Natural Hazards and Earth System Sciences* 5(4): 555–559.
- D. Malamud, B. & L. Turcotte, D. 1999. Self-affine time series: measures of weak and strong persistence. *Journal of Statistical Planning and Inference* 80(1–2): 173–196.
- Dachev, T.P. 2018. South-Atlantic Anomaly magnetic storms effects as observed outside the International Space Station in 2008–2016. *Journal of Atmospheric and Solar-Terrestrial Physics* 179: 251–260.
- Grigoryan, O.R., Romashova, V. V. & Petrov, A.N. 2008. SAA drift: Experimental results. *Advances in Space Research* 41(1): 76–80.
- Heirtzler, J.R. 2002. The future of the South Atlantic anomaly and implications for radiation damage in space. *Journal of Atmospheric and Solar-Terrestrial Physics* 64(16): 1701–1708.

- Huang, C.-S., Foster, J.C., Goncharenko, L.P., Reeves, G.D., Chau, J.L., Yumoto, K. & Kitamura, K. 2004. Variations of low-latitude geomagnetic fields and Dst index caused by magnetospheric substorms. *Journal of Geophysical Research* 109(A5): 1–14.
- Jalabert, E. & Mercier, F. 2018. Analysis of south atlantic anomaly perturbations on Sentinel-3A Ultra Stable Oscillator. Impact on DORIS phase measurement and DORIS station positioning. *Advances in Space Research* 62(1): 174–190.
- Jr, O.P. & Gonzalez, W.D. 1989. Energetic electron precipitation at the South Atlantic Magnetic Anomaly : a review. *Journal of Atmospheric and Terrestrial Physics* 51(5): 351–365.
- Jr, O.P., Gonzalez, W.D., Pinto, I.R.C.A., Gonzalez, A.L.C. & Jr, O.M. 1992. The South Atlantic Magnetic Anomaly : three decades of research. *Journal of Atmospheric and Terrestrial Physics* 54(9): 1129–1134.
- Koch, S. & Kuvshinov, A. 2015. Does the South Atlantic Anomaly influence the ionospheric Sq current system? Inferences from analysis of ground-based magnetic data. *Earth Planets and Space* 67: 1–7.
- Kozyra, J.U. & Liemohn, M.W. 2003. Ring current energy input and decay. *Space Science Reviews* 109: 105–131.
- Mohammed Hatem, Z., A. Kassem, M., Ali, K.N. & Khoiry, M.A. 2022. A new perspective on the relationship between the construction industry performance and the economy outcome- A Literature Review. *Jurnal Kejuruteraan* 34(2): 191–200.
- Muhammad, S. & Jamaludin, S.A. 2022. Evaluating the performance of traffic flow using SIDRA for Roundabouts in Ipoh, Perak. *Jurnal Kejuruteraan* 34(3): 421–427.
- Naser, A.F. 2022. A review study on theoretical comparison between time-dependent analysis models for prestressed concrete bridges. *Jurnal Kejuruteraan* 34(3): 375–385.
- Nasuddin, K.A., Abdullah, M. & Abdul Hamid, N.S. 2019. Characterization of the south atlantic anomaly. *Nonlin. Processes Geophys.* 26(1): 25–35.
- Oladeji Araoyinbo, A., Bose Edun, M., Ushe Samuel, A., Rahmat, A., Biola Biodun, M. & Albakri, M.M. 2022. Influence of cutting fluid on machining processes: A Review. *Jurnal Kejuruteraan* 34(3): 365–373.
- Panchev, S. & Tsekov, M. 2007. Empirical evidences of persistence and dynamical chaos in solar-terrestrial phenomena. *Journal of Atmospheric and Solar-Terrestrial Physics* 69(17–18): 2391–2404.
- Papa, A.R.R. & Sosman, L.P. 2008. Statistical properties of geomagnetic measurements as a potential forecast tool for strong perturbations. *Journal of Atmospheric and Solar-Terrestrial Physics* 70(7): 1102–1109.
- Samuel Omoniyi, S., Olufemi Odufuwa, B. & Osarumwense Uzzi, F. 2022. Residents' perception of housing quality index for Dwellings' physical characteristics in the Core Area of Ado-Ekiti, Nigeria. *Jurnal Kejuruteraan* 34(2): 223–230.
- Schaefer, R.K., Paxton, L.J., Selby, C., Ogorzalek, B., Romeo, G., Wolven, B. & Hsieh, S.-Y. 2016. Observation and modeling of the South Atlantic Anomaly in low Earth orbit using photometric instrument data. *Space Weather* 14(5): 330–342.
- Willis, P., B. Heflin, M., J. Haines, B., E. Bar-Sever, Y., I. Bertiger, W. & Manda, M. 2016. Is the Jason-2 DORIS oscillator also affected by the South Atlantic Anomaly? *Advances in Space Research* 58(12): 2617–2627.
- Zaourar, N., Hamoudi, M., Holschneider, M. & Manda, M. 2013. Fractal dynamics of geomagnetic storms. *Arabian Journal of Geosciences* 6: 1693–1702.
- Zou, H., Li, C., Zong, Q., K. Parks, G., Pu, Z., Chen, H., Xie, L. & Zhang, X. 2015. Short-term variations of the inner radiation belt in the South Atlantic anomaly. *Journal of Geophysical Research: Space Physics* 120(6): 4475–4486.